

# Numerical Simulations in SCR systems with Emphasis on Uniform Flow at the Catalyst Inlet

*Martin Novák*<sup>1\*</sup>, *Richard Matas*<sup>2</sup>

<sup>1</sup>Department of Power System Engineering, Faculty of Mechanical Engineering, University of West Bohemia, Univerzitní 2762/22, 301 00 Pilsen, Czech Republic

<sup>2</sup>Modelling and Simulations in Technical systems, New Technologies – Research Centre, University of West Bohemia, Univerzitní 2732/8, 301 00 Pilsen, Czech Republic

**Abstract.** Selective Catalytic Reduction (SCR) is one of the most widely used technologies for reducing emissions from diesel engines, which are widely used in the energy world. This technology is very complex, and it is not currently possible to address all aspects of it comprehensively. This study focuses on trying to improve the distribution of the exhaust stream at the catalyst inlet using models which represent the most common geometric distributions. Four types of geometries are selected, complemented by a fifth design, which is used as a reference, to find the maximum achievable values of the parameters under study. In this case, mainly the uniformity index is addressed, which indicates how uniformly the selected variable is distributed over the particular area. The study presents possible modifications of the flue gas duct which will be generally applied.

## 1 Motivation

It is essential to design an SCR system well, to meet requirements such as sufficient residence time of the injected AdBlue® and subsequent even distribution of ammonia at the catalyst inlet. Very often the system is not well designed, and geometry changes are needed to improve its functionality. As far as possible, efforts are made to minimise interference with the system design. A successful example of a simple geometry change was made by Li et al. who achieved the desired change by only slightly modifying the blades already in use. [1] Another example of a simple modification to the flue was made by Mi et al. who added vanes to the duct to provide better ammonia distribution. [2] Hong et al. also improved the flow in the duct by a similar change in geometry. [3]

Another commonly used component is a Static Axial Rectifier. It increases the effectiveness of the SCR system as reported by Mehdi et al. [4] They increased the effectiveness by increasing the dwell time of the droplets in the manifold, which results in higher evaporation and therefore higher effectiveness. Another reason for the higher effectiveness is that the heat transfer to the droplets is also increased due to increased turbulence, therefore the droplets evaporate faster. These claims are confirmed by Tan et al. in their publication. [5] Several interesting designs of rectifier modules are described by Xu

---

\* Corresponding author: [novakm42@ntc.zcu.cz](mailto:novakm42@ntc.zcu.cz)

et al. It should also be pointed out that the distance to evaporation in their SCR system is very small, so one cannot expect the injection fluid to completely evaporate before entering the catalyst. However, the effectiveness of the system is still increased when using the modules. [6] There are other articles also confirming the improvement of the system function, see [7] [8] [9].

Modelling a catalyst is a complex matter as it consists of a huge number of small channels, so it is common to simplify this part of the model in CFD simulation by using a porous medium. This simplification has no significantly negative effects on the results. A comparison between an ANSYS Fluent simulation and an experiment is described by Holtz et al. [10] and indicates that the results are comparable.

Experimental validation of the calculations has been carried out, for example, by Wardana et al. [11] Their research involved the chemical reactions and evaporation process of a solution of water and urea. In their study, they investigated mixers for better mixing and increased conversion of the solution to ammonia. 3D simulations supported by their own experimental results were also reported by Luo et al [12]. They used the simplest reduction equations in the flue gas stream in their research, but they also considered the chemical processes in the catalyst, which they simplified by using a porous medium. They compared stationary and non-stationary approaches to the calculations and concluded that the results are similar. A comprehensive approach to 3D CFD simulation of an SCR system was taken by Lee [13] in his study. He included the evaporation process, thermolysis and hydrolysis of urea (water and urea solution), the aqueous film and the effect of the mixer on the overall system in his calculations. He compared the calculations with experiments and found very good agreement. He also investigated changing the position of the solution injection and the insertion of mixers into the flue gas stream. Zhang et al. [14] proposed very interesting mixers in the exhaust duct which included droplet evaporation, a water film on the mixer walls and chemical processes related to SCR. They verified their results experimentally.

The application of an SCR system in ship engines was investigated by Mehdi et al. [4], who also concluded that it is advisable to use mixers in the exhaust duct to improve the flow. This is only a numerical simulation without experimental verification. SCR systems can be applied on different devices, for example, Gao et al. [15] performed numerical simulations and an experiment on a flue downstream of a gas turbine. They used the three most common equations describing the chemical reactions of selective catalytic reduction and concluded that the results were equivalent.

All these studies consider a uniform input profile to the SCR technology. In addition, different inlet profiles are not used, which would establish the sensitivity of the system to different inlet parameters (velocity profiles). For most SCR systems, it can be assumed that the exhaust gas passes through a turbocharger that does not have a uniform exit profile at the outlet. Therefore, a small part of the study presented here will also point out the fact that different inlet profiles play a role. Because then one could argue whether the internal inserts, which are very popular for improving the effectiveness of these systems, are generally applicable or only applicable to the one particular case.

## 2 Geometry

It can be seen from the previous chapter that the design of an SCR device, whether it is a CHP unit or a large engine, can be divided into several basic designs. These are illustrated in Figure 1. In the following Figures 1, 2 and 3 are inlets displayed by blue arrows and outlets by red arrows.

The first is to place the catalyst behind the engine via two 90° elbows. The second solution has only one elbow. Variants one and two have the same length of pipe in front of the catalytic converter. In the first case, the pipe is divided by means of elbows into three

equal length units. In the second design, the pipe is split in half. The next option for the location of the SCR catalyst is similar to the second option, except that the elbow is straight into the catalyst, i.e. there is no straight pipe beforehand to further direct the flow after the elbow. The fourth geometric solution, which was used in some cases mentioned in the previous chapter, is shown at the bottom right. This geometry is mainly chosen in designs where a compact design of the whole system is required. The fifth variant, shown here, serves as a reference. It is not a geometry that would be applicable in a real design, because building requirements usually do not allow a straight supply pipe. This variant serves as the basis for the set of variants shown in Figure 1. These variants are shown with the same type of catalyst, which has a circular cross section. This type of catalyst has already been used in [16], therefore it is considered to be a realistic model.

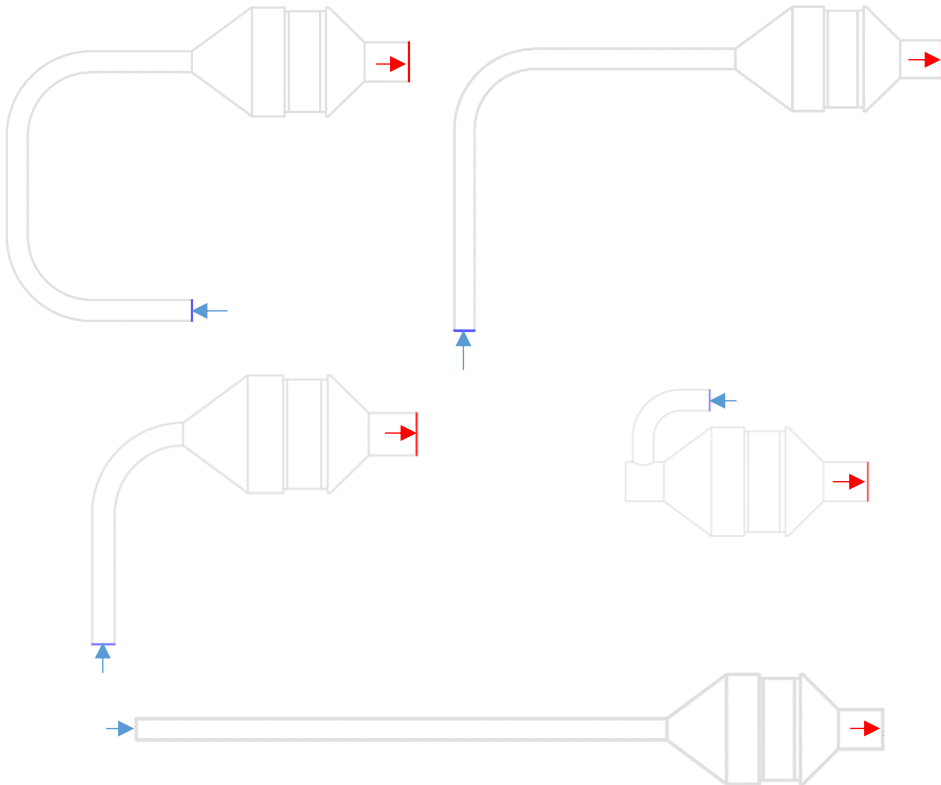


**Fig. 1** a) upper left – variant “double\_knee”, b) upper right – variant “long\_knee”, c) middle left – variant “short\_knee”, d) middle right – variant “tdm”, e) down – variant “straight”

Based on the reference variant, the set of variants represented here by only three geometries aims to determine the appropriate shape of the inlet chamber into the catalyst are shown in Figure 2. This set of variants includes changing the angle of the inlet chamber in  $5^\circ$  increments, up to  $80^\circ$ , and then changing the angle in  $1^\circ$  increments. The first variant has an angle of attack of  $0^\circ$ , the second geometry has an angle of attack of  $30^\circ$ , and the last model has an angle of attack of  $85^\circ$ .



**Fig. 2** a) top – variant “straight\_0deg”, b) middle – variant “straight\_30deg”, c) down – variant “straight\_0deg”,

This set of variants essentially modifies the inlet to the catalyst and turns it into a diffuser where the pressure/velocity ratio is changed. This geometric modification can be used for all the other variants as well, since the results from the straight pipe indicate that changing the geometry in this direction is desirable, as it results in a more uniform flow and a better distribution of the flow field at the catalyst inlet.

A large number of geometric variations have been developed; therefore, only representative samples are shown here. In Figure 3 at the top left, a modified variant with two elbows is shown, but the pipe expansion starts from the inlet. At the top right, in the same figure, a similar variant is shown, i.e., the pipe diameter expands from the inlet, but the first elbow is rotated by 180°. The bottom left shows the same variant as the two previous ones, with two elbows, but the pipe widens at the end of the second elbow. The last of the variants in this figure is the 'TDM' variant with the inlet modified so that the pipes are connected by a T-piece rather than an elbow.

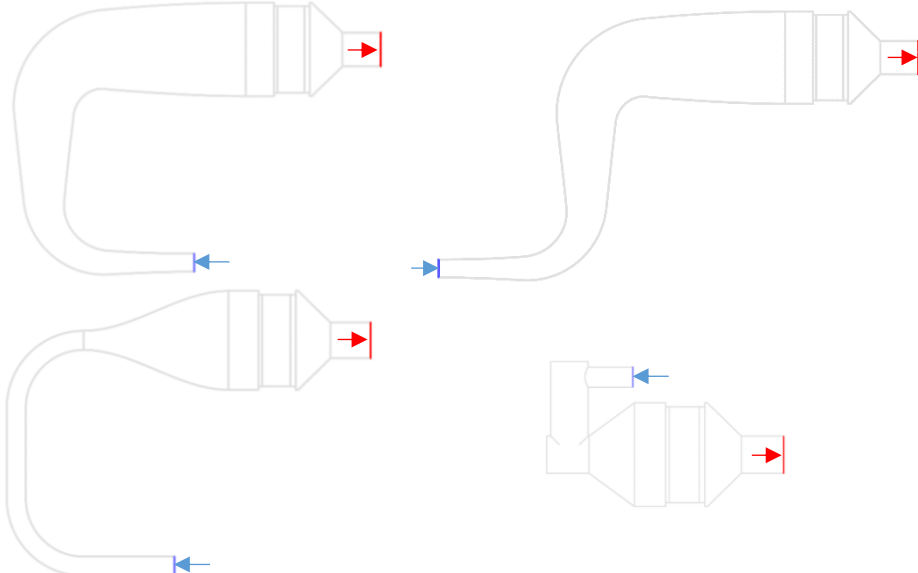


**Fig. 3** a) upper left – variant “double\_knee-cone”, b) upper right – variant “double\_knee-cone-rot”, c) lower left – variant “double\_knee-third-cone”, d) lower right – variant “tdm-tupo-bigst”

As mentioned above, more than fifty geometric variations were designed. The variants with “cone” suffix were designed because ANSYS Fluent and its "Adjoint Solver" optimization function started to change the diameter of the inlet pipe. However, the program did not achieve any major changes in the flow with these modifications, as the computation time was considerable, and the rate of change was small. Therefore, the pipe diameter was changed manually for the straight inlet pipe variant and the other geometric variants were further modified.

The other variants are derived from the “double\_knee” and “long\_knee” types where the pipe diameter is changed. In addition, we designed variants of these two types with different elbow radiuses to investigate the effect of the parameters on the flow in the catalyst inlet chamber.

### 3 Simulation description

Fluid mechanics tries to find the values of four basic quantities. These are pressure  $p$ , velocity  $w$ , temperature  $T$  and density  $\rho$ . Three physical laws are used to solve these unknowns. The first is the law of conservation of momentum, the second is the law of conservation of mass, and the third is the law of conservation of energy. Density is considered to be constant, so the fourth equation is not necessary to solve the system of equations

The law of conservation of momentum is represented by the Navier-Stokes equations, which are analytically solvable only in exceptional cases and therefore we solve them numerically. Momentum is a vector, so it is broken it down into three components. [17]

$$\frac{\partial u}{\partial t} + \frac{\partial(uu)}{\partial x} + \frac{\partial(uv)}{\partial y} + \frac{\partial(uw)}{\partial z} = -\frac{1}{\rho} \frac{\partial p}{\partial x} + \nu \left( \frac{\partial^2 u}{\partial x^2} + \frac{\partial^2 u}{\partial y^2} + \frac{\partial^2 u}{\partial z^2} \right) + f_x \quad (1)$$

$$\frac{\partial v}{\partial t} + \frac{\partial(vu)}{\partial x} + \frac{\partial(vv)}{\partial y} + \frac{\partial(vw)}{\partial z} = -\frac{1}{\rho} \frac{\partial p}{\partial y} + \nu \left( \frac{\partial^2 v}{\partial x^2} + \frac{\partial^2 v}{\partial y^2} + \frac{\partial^2 v}{\partial z^2} \right) + f_y \quad (2)$$

$$\frac{\partial w}{\partial t} + \frac{\partial(wu)}{\partial x} + \frac{\partial(wv)}{\partial y} + \frac{\partial(ww)}{\partial z} = -\frac{1}{\rho} \frac{\partial p}{\partial z} + \nu \left( \frac{\partial^2 w}{\partial x^2} + \frac{\partial^2 w}{\partial y^2} + \frac{\partial^2 w}{\partial z^2} \right) + f_z \quad (3)$$

In equations (1) - (3),  $u, v, w$  represent the individual velocity components in the  $x, y, z$  direction.  $t$  is time,  $p$  is pressure and  $\rho$  is the density of the fluid. The kinematic viscosity is denoted by  $\nu$ . Since this is an equation based on the laws of physics, it is possible to determine what each term means. The first product represents the acceleration of the fluid (local), and the next three terms represent the nonlinear internal inertial acceleration. These terms cause instabilities at higher Reynolds numbers. The first term on the right side represents the pressure gradient (inertial acceleration due to pressure). The next term is the acceleration from the shear stresses of the fluid caused by its viscosity. The last terms  $f_x, f_y, f_z$  are the components of the external volumetric accelerations. All terms have a dimension of acceleration. If it is necessary to write the equation in terms of forces, both sides can just be multiplied by the mass. [17] [18]

The law of conservation of mass describes the continuity equations. When considering density as invariable, the equation takes the following form:

$$\frac{\partial u}{\partial x} + \frac{\partial v}{\partial y} + \frac{\partial w}{\partial z} = 0 \quad (4)$$

As in the Navier-Stokes equation, the velocity components  $u, v, w$  are in the three  $x, y, z$  directions. What is interesting about this equation is that the right side of the equation is 0. The left side of the equation must be zero because the amount of fluid entering the control volume is assumed to be the same as the amount that flows out of that volume. [17]

The law of conservation of energy is defined by the energy equation. This equation, for a constant density  $\rho$ , is discussed in the following lines. For clarity, substitution by  $\psi$  has been used, otherwise the equation would be long, and not entirely clear.

$$\frac{\partial T}{\partial t} + \frac{\partial(uT)}{\partial x} + \frac{\partial(vT)}{\partial y} + \frac{\partial(wT)}{\partial z} = \alpha \left( \frac{\partial^2 T}{\partial x^2} + \frac{\partial^2 T}{\partial y^2} + \frac{\partial^2 T}{\partial z^2} \right) + \mu \psi \quad (5)$$

$$\psi = 2 \left( \left( \frac{\partial u}{\partial x} \right)^2 + \left( \frac{\partial v}{\partial y} \right)^2 + \left( \frac{\partial w}{\partial z} \right)^2 \right) + \left( \left( \frac{\partial u}{\partial y} + \frac{\partial v}{\partial x} \right)^2 + \left( \frac{\partial u}{\partial z} + \frac{\partial w}{\partial x} \right)^2 + \left( \frac{\partial v}{\partial z} + \frac{\partial w}{\partial y} \right)^2 \right) \quad (6)$$

$$\alpha = \frac{\lambda}{\rho \cdot c_p} \quad (7)$$

In equations (5) - (7), T represents the thermodynamic temperature; t is time;  $u, v, w$  are the velocity components;  $\alpha$  is the thermal conductivity coefficient;  $\lambda$  is the thermal conductivity coefficient;  $\rho$  is the density;  $c_p$  is the specific heat capacity at constant pressure;  $\mu$  is the dynamic viscosity. The first term in Equation 5 describes the heat accumulation in the liquid. The remaining terms on the left side of the equation represent convection caused by flow. The first term on the right side represents heat conduction. The last term, which is subsequently broken down, represents the heat from the deformation and movement of the fluid. [17] [19]

The calculation program was ANSYS Fluent [20]. The simulations were performed as stationary, the turbulence model was SST  $k-\omega$  [21]. As mentioned above, the input velocity profile is not uniform. The input profile has already been described in a previous paper, which is the logical predecessor of this paper [16]. In the introduction of this text, it is mentioned that modelling the catalyst as a geometrically complex component is possible by using a porous zone that can replace the behaviour of the real component, so this simplification was also adopted in this case. In order to achieve this simplification, it was necessary to create a submodel of a realistic part of the catalyst. The pressure drop was determined from it and then the corresponding values were set in the porous zone accordingly.

## 4 Results

The Uniformity Index (UI) is one of the most commonly used parameters in evaluating the uniformity of the input field to the catalyst. This index was first introduced by Weltens et al. in 1993 in their paper dealing specifically with the distribution of the flow field upstream of an SCR catalyst inlet. [22] This index has proven to be an important variable for the quantitative assessment of uniform velocity field distribution. [23] Bressler et al. state that a series of experiments confirm the need to ensure a homogeneous velocity field distribution at the catalyst inlet, because this will ensure a longer lifetime and lower pressure losses. [24] In addition, the NOx conversion effectiveness will be increased, and the ammonia slip, which is also an emission, will be reduced. [25] [26] UI can be used to evaluate variables other than velocity. For example, Capetillo et al. used it to evaluate the uniformity of ammonia distribution, and Vedagiri et al. used it when evaluating concentrations. [27] [28]

The calculation of the UI index is given in equation (8) as reported by Girard et al., or Johansson et al., [29] [30]

$$UI = 1 - \frac{1}{2} \cdot \frac{\sum_{i=1}^n (|v_i - v_{mean}| \cdot A_i)}{A \cdot v_{mean}} \quad (8)$$

where  $v_i$  [m/s] is the velocity at the local location (cell),  $v_{mean}$  [m/s] is the mean velocity over the evaluation area,  $A_i$  [m<sup>2</sup>] is the area at the local location (cell area) and  $A$  [m<sup>2</sup>] is the total size of the evaluation area.

The value of this index is between 0 and 1. At a value of 1 the field is completely uniform, which means the value of the variable is the same in each location (cell). [29] Weltens et al. state that for a fully developed flow in a tube of  $Re = 64000 [-]$ , the value of  $UI = 0.94 [-]$ . [22] Lu et al. state that the UI of the velocity field needs to be at least  $0.98 [-]$  to ensure maximum catalyst effectiveness. [25] Kurzydym et al. state that a UI value of  $\geq 0.94 [-]$  can be considered as a good result. [9] However, all the authors of publications related to this topic aim for the highest possible value of the uniformity index in their studies.

The uniformity index can be weighted by the mass flux in addition to weighted by the area, see equation (8). Both options are implemented in ANSYS Fluent using equations (9) to (12). The area-weighted UI is denoted as  $\gamma_a$  for the computed variable  $\phi$ .

$$\gamma_a = 1 - \frac{\sum_{i=1}^n [(\phi_i - \overline{\phi_a}) A_i]}{2|\overline{\phi_a}| \sum_{i=1}^n A_i} \tag{9}$$

$$\overline{\phi_a} = \frac{\sum_{i=1}^n \phi_i A_i}{\sum_{i=1}^n A_i} \tag{10}$$

Where  $i$  is the area index of an area composed of  $n$  faces and  $\phi_a$  is the area-weighted average value of the variable. In the following lines,  $\gamma_m$  is the area-weighted UI and  $\phi_m$  is the average value of the variable weighted by the mass flux.

$$\gamma_m = 1 - \frac{\sum_{i=1}^n [(\phi_i - \overline{\phi_m})(\rho_i \overline{v}_i A_i)]}{2|\overline{\phi_m}| \sum_{i=1}^n [|\rho_i \overline{v}_i A_i|]} \tag{11}$$

$$\overline{\phi_m} = \frac{\sum_{i=1}^n [\phi_i (\rho_i \overline{v}_i A_i)]}{\sum_{i=1}^n [|\rho_i \overline{v}_i A_i|]} \tag{12}$$

The uniformity index is an important parameter in this study and is one of the most important indicators for evaluating the quality of the design variant at this stage of the calculations, as it eliminates clearly unsuitable options.

The first results presented here are the straight pipe variants where only the angle (size) of the catalyst inlet chamber is changed, see Figure 4. The graph in Figure 4 contains two sets of results, which are composed of four different velocities -  $70 [m/s]$ ,  $120 [m/s]$ ,  $171 [m/s]$  and  $210 [m/s]$ . One result shows the UI mean drifting velocity (only the velocity towards the catalyst) weighted by mass flow (UI MW - Uniformity Index Mass flow Weighted) and the other results are area weighted (UI AW - Uniformity Index Area Weighted). At first sight, the UI values vary depending on what they are averaged over. There are no consistent variations until above  $80^\circ$ , until then it can be clearly said that the more conservative UI values are represented by the area weighting, so those values will continue to be considered.

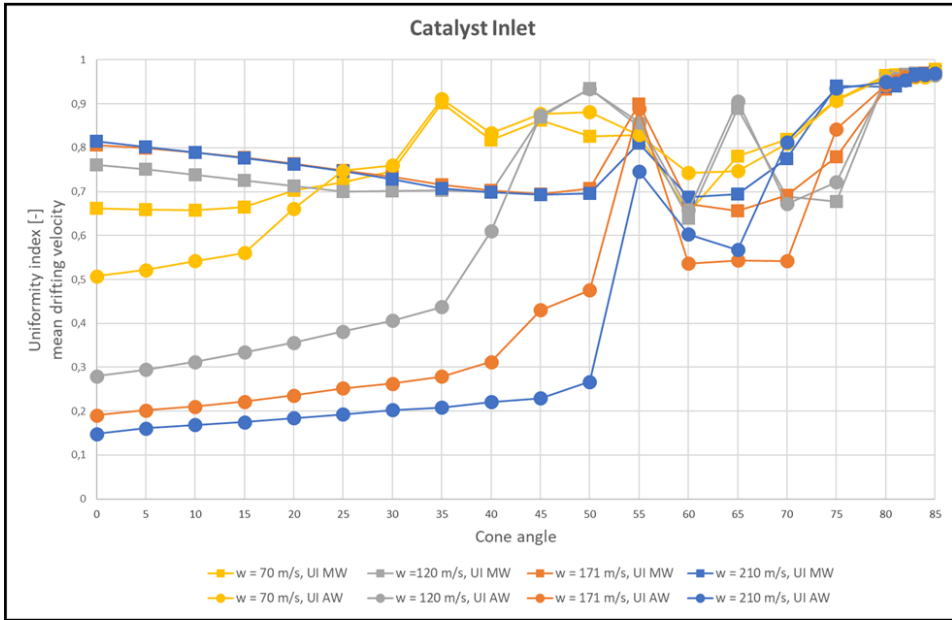


**Fig. 4** UI mean drifting velocity –“straight” variant

It is mentioned above that it is necessary to achieve the highest possible UI value, ideally values above 0.94 (better above 0.98). In this case, these values are achieved above an angle of 80°, with the UI MW and UI AW values being identical only at angles greater than and including 83°.

Another important factor to observe is the ratio of the area of the drift velocity (in the direction of flow) to the total area. This parameter tells how much flow is in that direction or how much is not flowing there (backflow, stalling, perpendicular flow, etc.). The values of this variable are shown in Figure 5. It can be seen that at lower velocities the flow is stable, and everything flows in one direction. At increasing velocities and small angles, the flow is concentrated only in one part (the middle part) of the catalyst and in other parts the flow is rotating in the inlet chamber. Therefore in some situations ( $w = 210 [m/s]$ ) the value of the area ratio is less than 0.5, which means that the flow direction is mostly towards the catalyst. At higher angles, as in the previous case above 80°, or 83°, the area ratio is equal to one, meaning that there is flow in one direction (into the catalyst) throughout the channel.



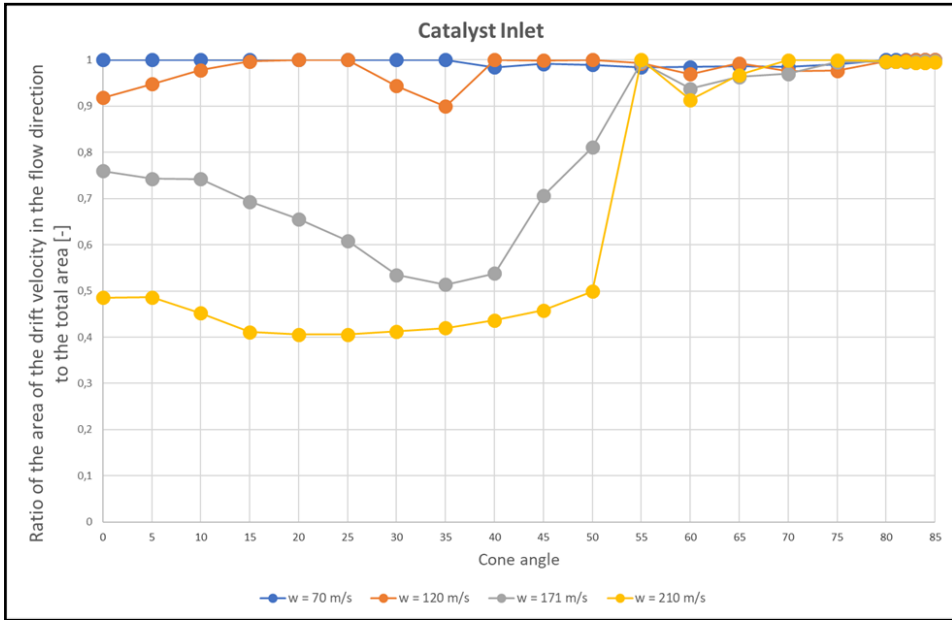
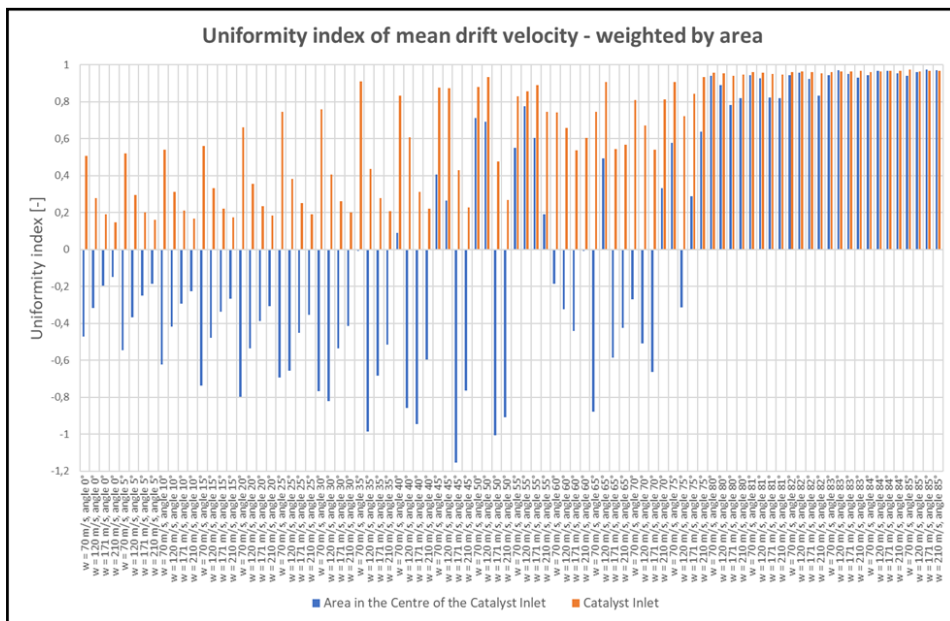


Fig. 5 Area ratio, “straight” variant

The uniformity index is supposed to take values between 0 and 1. However, in some special cases, according to all available data, it has other values. See Figure 6, where it can be seen that the UI values are not only negative but also greater than one (if absolute values are taken). The negative values are due to the fact that the flow is complex and it flows in more directions than just the catalyst axis direction (drift direction), or there is also backflow in a large part of the channel, which is undesirable. These negative values are recorded on a surface that is in the middle of the straight part of the inlet chamber, so that it is equidistant from the catalyst inlet for all variants. It can be seen that in this section the backflow is significant and affects the UI evaluation. But looking at the area in the catalyst inlet, the UI is already evaluated correctly and does not take on values that can be claimed as erroneous.

Because of the way UI behaves, this factor should only be used in areas (locations/ cross-sections) where there is a clear direction of flow and problematic backflow is not occurring to any significant degree. Therefore, below we only deal with the evaluation of the UI at the catalyst inlet, where there is no introduction of inappropriate values into the evaluation.



**Fig. 6** Uniformity index of mean drift velocity – weighted by area, “straight” variant

The above results are for the reference variant and are used to assess the behaviour of the system and to prepare a suitable apparatus for comparison. It is also used to determine the potentially best possible value of the area to UI ratio, which can be expected to be the best possible for a straight pipe, as the geometry is not affected by any negative effects in the form of elbow (drift behind these elements).

Figure 7 contains the results from the "other" variants. These variants have already been roughly outlined in the introduction of this chapter, but here it can be clearly seen that there are many more variants solved than mentioned above. However, all the variants are based on the four basic ones - "double\_knee", "long\_knee", "short\_knee" and "tdm", plus some results for the "straight" variant where certain parameters are changed.

The results in the figure show the ratio of the drift velocity area to the total area at the catalyst inlet. Here, it is necessary to point out the range of the area ratio, which does not start at 0, but with a value of 0.5. However, results with an area ratio below 0.85 can be evaluated as inappropriate since, even at this value, 15% of the area is backflowing, or 15% of the catalyst area is not used.

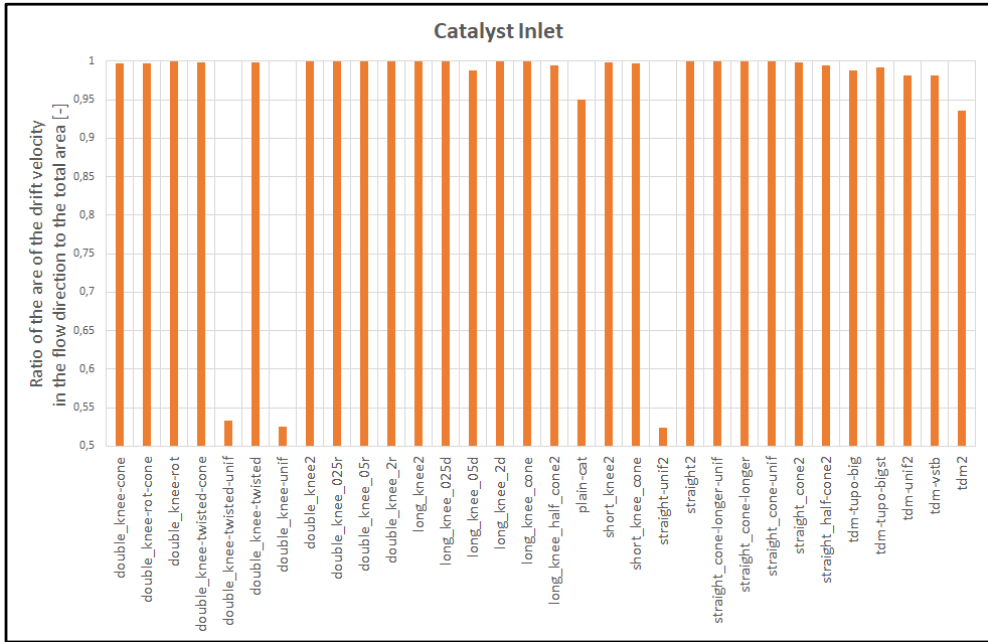


**Fig. 7** Area ratio, remaining variants

The second criterion for selecting a suitable solution is the UI. The variants mentioned above are evaluated with respect to UI in Figure 8.

The result of the basic variant "tdm" is "tdm2". It does not achieve the highest UI values, which can be clearly seen from the results. Several variants of geometry modifications are designed and it can be seen that the variant "tdm-tupo-bisgt", which has a 34% higher UI value over the basic variant. The second best geometric design for this option is "tdm-vstb". However, it contains an insert that may be susceptible to damage, and these kinds of modifications will be further addressed in follow-up research. When comparing the "tdm2" and "tdm-unif2" variants, which differ only in their inlet velocity profiles, it can be seen that the velocity distribution at the catalyst inlet needs to be addressed as this also has a significant impact on the UI.

The "straight" variants have already been largely covered in the previous section, which dealt with changing the angle of the inlet chamber to the catalyst. These variants are here referred to as "straight" + "cone". However, here it is useful to compare two variants, namely, "straight2" and "straight-unif2". These differ only in the distribution of the inlet velocity (velocity profile), where the "straight-unif2" variant has a uniform inlet. Here a significant dependence on the inlet profile can be seen, as the UI differs by 42% in this case, so the dramatic change in velocity distribution has a significant effect on how uniform the flow is at the catalyst inlet.

There are only two examples of "short\_knee" variants given here. The difference between this variant and the "long\_knee" variant can be seen at the beginning of this text in the section describing the geometry. Comparing the two results, it can be clearly seen that by changing the geometry of the pipe to an expanding pipe (cone/cone shape), there is a 32% change in UI.

The "long\_knee" set of variants also has many derivatives. Variants with the "d" suffix contain a different elbow radius from the original radius (it varies proportionally according to the values given before the "d" suffix). The change to a larger radius is positive, the change to a smaller radius is negative. The original "long\_knee" variant achieved a significant

improvement in UI of 30% after the geometry change, called the "long\_knee\_cone" variant, by using an expanding pipe diameter.

The original variant "double\_knee2" is the default variant for the last set of geometries shown in the following figure, reaching the highest UI value. This seems to be a unique issue, as any intervention in the geometry has a negative effect on the flow, so a stable solution to the problem needs to be found. Variants containing the "unif" suffix are those that contain a uniform inlet profile and at first glance appear to achieve the lowest values. This is the last piece of evidence that the inlet profile fundamentally affects the UI. It is clear from the results that the highest values of uniformity are achieved when an expanding pipe, the "cone" extension, is used. It does not matter whether both elbows are bent in the same direction, as the variants containing the "rot" have one original elbow and the other rotated 180° when the pipe is expanded. So, when comparing the "double\_knee\_cone" and "double\_knee\_rot\_cone" variants, it can be seen that the results are almost identical. Some variants are calculated with only the shorter extension section of the pipe, but these do not achieve as high UI values as those with the full extension pipe.

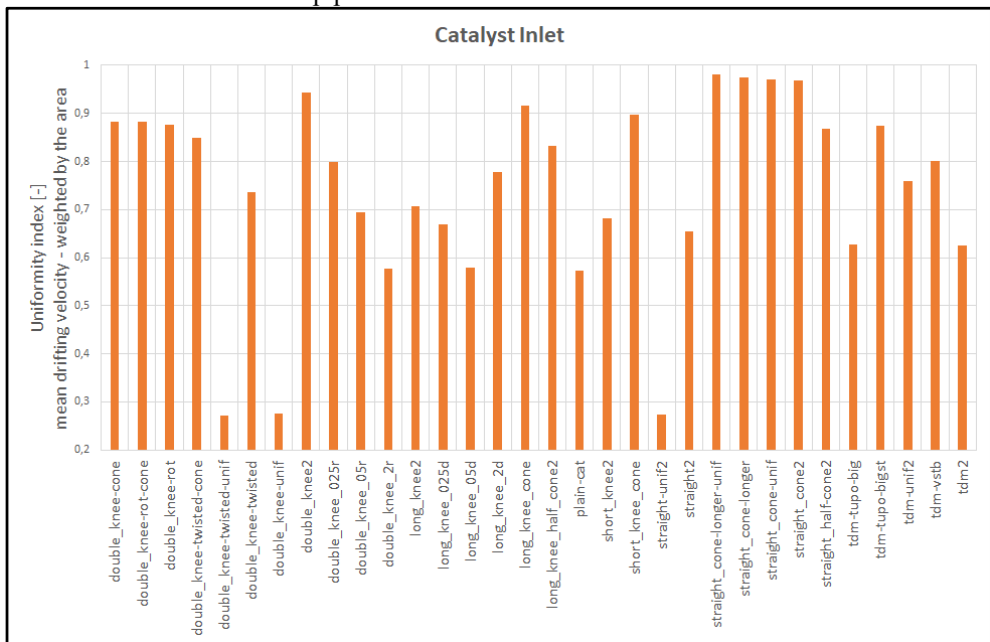


**Fig. 8** UI mean drifting velocity – rest of the variants

Another variable that can indirectly affect UI is the diameter of the pipe and the radius of the elbows. The radius of the elbows has been mentioned above, and the following figure shows the results from these calculations. The results are for the larger pipe diameter, which in this case is 106.5 [mm] (the original pipe diameter is 71 [mm]). From these results at low velocities (70 [m/s]) the UI is minimally affected, when the radius of the elbows is changed. In the other cases, a clear trend can be seen that the UI increases with increasing radius. These values can be compared with those in the previous figure and a larger pipe diameter in this case negatively affects the UI.

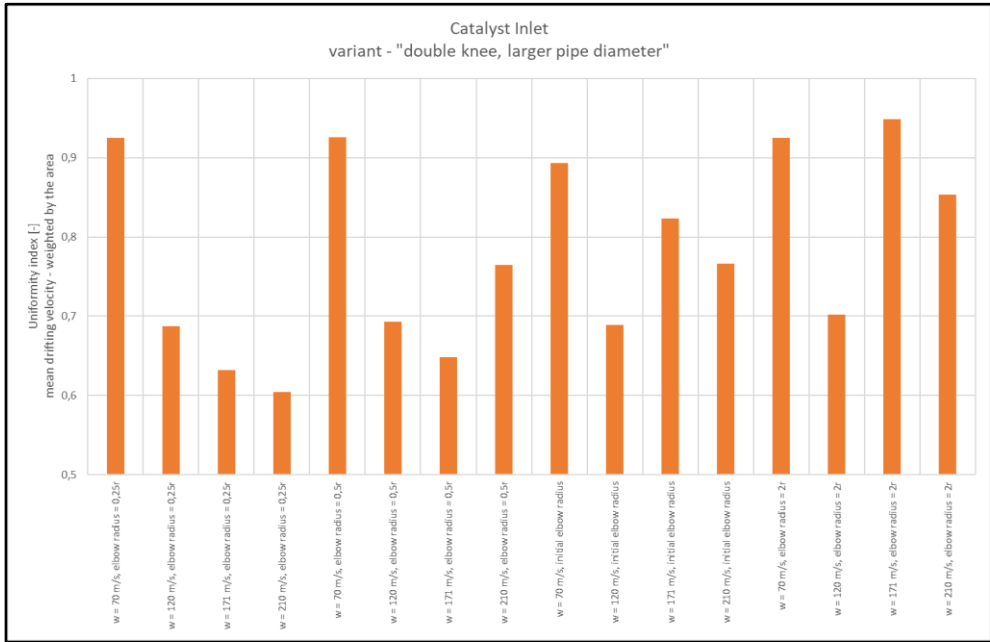


**Fig. 9** UI, variant "double\_knee"

The "long\_knee" variant was modified in a similar way to the "double\_knee" variant (in the previous figure), i.e., the diameter of the pipe was increased and the radius of the elbow was changed. It is not possible to clearly see what trend is occurring here. For the highest and lowest velocities, it can be seen that the UI value increases as the radius of the elbows increases, however, for the middle velocities (120 [m/s] and 171 [m/s]) this is not the case, and the UI decreases as the radius of the elbow increases. It is clear that the larger diameter has a positive effect on the UI value in this case.

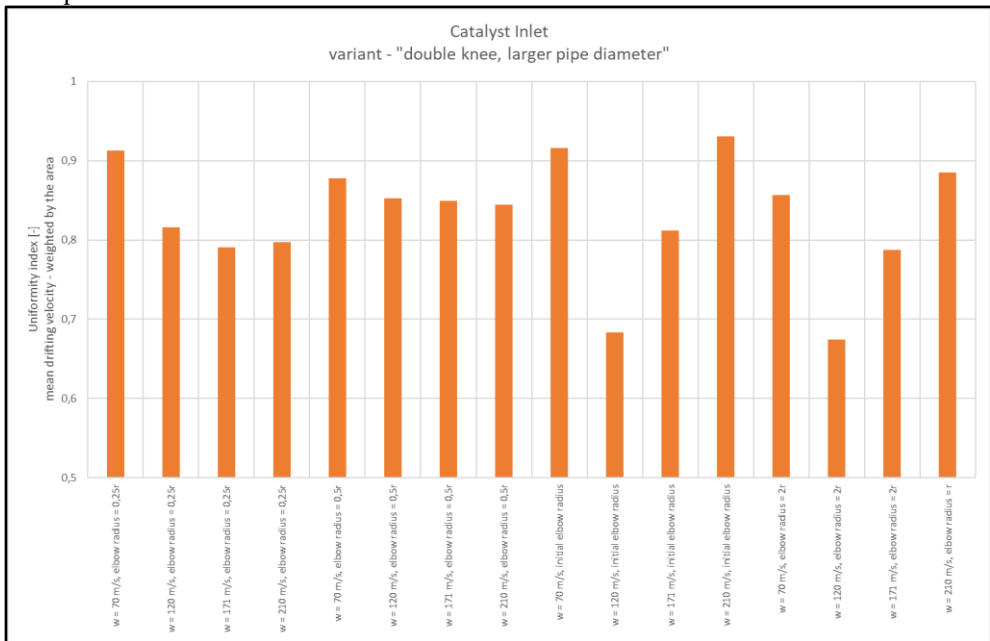


**Fig. 10** UI, variant "long\_knee"

## 5 Conclusion

Selective catalytic reduction is an important topic which is relevant, as reducing emissions is an important aspect for the survival of society and the planet. Therefore, we need to keep improving these systems to achieve the best results and highest effectiveness using the best available technologies, which are becoming more sophisticated every year. CFD simulations includes a lot of physical phenomena and since these are simulations it is always necessary to think about whether the results make sense and are physical. Experience in fluid mechanics gained through previous projects is needed to assess whether the results are meaningful. And even that it is always great to make experiments which proves the CFD results, but it is not possible to do it in this case because there is a plenty of geometrical modifications and only the best one deserves to be tested since manufacturing the pipeline costs time and money.

The present work deals with the modification of the catalyst inlet duct in order to increase the utilized area of the catalyst and at the same time to make the distribution of the exhaust stream on it as uniform as possible. For this purpose, two parameters are presented - the ratio of the drift velocity area to the total area, and the uniformity index. However, this index is only applicable in cases where the flow is in one direction without significant eddies and backflow effects.

The best options for solving the issue seem to be those where the pipe gradually increases its cross-section up to the diameter of the catalyst inlet chamber. These variants are "double\_knee-cone", "short\_knee\_cone" "long\_knee\_cone" and "tdm\_tupo\_bigst". However, even derivatives of these variants, which have a shorter cone section, reach quite good values. So, according to the available data, it is clear that these changes also improve the situation at the catalyst inlet.

The next line of research will focus on further increasing the UI by using the internal inserts which are briefly mentioned in this paper. The next steps of research in this area will look at variants into which droplets of aqueous urea solution fluid will be injected, along with evaporation. The distribution (UI) of this evaporated second phase at the catalyst inlet will be monitored. The next step will involve solving the basic chemical equations that are integral to SCR technology. Once the simulations show a significant improvement to a real-life SCR system then the experiment will be conducted on that particular engine.

## Acknowledgments

This work was financially supported by student project SGS-2022-023 (Research and development of power machines and equipment).

## References

1. LI, Mao, Hongjie YAN a Jiemin ZHOU. Numerical Simulation and Optimization of Flow Field in the SCR Denitrification System. In: *2009 International Conference on Energy and Environment Technology* [online]. IEEE, 2009, s. 415-418 [cit. 2022-04-26]. ISBN 978-0-7695-3819-8. Available from: doi:10.1109/ICEET.2009.565
2. MI, Jia, Dan A. PITSKO a Tim HASKEW. CFD Applications on Selective Catalytic NO<sub>x</sub> Reduction (SCR) Systems. In: *Volume 1:*

- Fora, Parts A, B, C, and D* [online]. ASMEDC, 2003, s. 2139-2146 [cit. 2022-04-26]. ISBN 0-7918-3696-7. Available from: doi:10.1115/FEDSM2003-45436
3. HONG, Wen Peng, Hao Shu DING a Yue HUANG. Numerical Simulation and Optimization of the Flow Field in the SCR System. *Advanced Materials Research* [online]. 2013, **860-863**, 1464-1469 [cit. 2022-04-26]. ISSN 1662-8985. Available from: doi:10.4028/www.scientific.net/AMR.860-863.1464
  4. MEHDI, Ghazanfar, Song ZHOU, Yuanqing ZHU, Shafquat HUSSAIN a Arif HUSSAIN. A CFD analysis of static mixer to study its impacts on SCR performance in marine diesel engine. In: *2019 2nd International Conference on Computing, Mathematics and Engineering Technologies (iCoMET)* [online]. IEEE, 2019, s. 1-6 [cit. 2022-04-26]. ISBN 978-1-5386-9509-8. Available from: doi:10.1109/ICOMET.2019.8673421
  5. TAN, Ligang, Pengfei FENG, Shubao YANG, Yage GUO, Shaochun LIU a Ziwen LI. CFD studies on effects of SCR mixers on the performance of urea conversion and mixing of the reducing agent. *Chemical Engineering and Processing - Process Intensification* [online]. 2018, **123**, 82-88 [cit. 2022-04-26]. ISSN 02552701. Available from: doi:10.1016/j.cep.2017.11.003
  6. XU, Zhengxin, Jingping LIU a Jianqin FU. Experimental investigation on the urea injection and mixing module for improving the performance of urea-SCR in diesel engines. *The Canadian Journal of Chemical Engineering* [online]. 2018, **96**(6), 1417-1429 [cit. 2022-04-26]. ISSN 00084034. Available from: doi:10.1002/cjce.23082
  7. QU, Litao, Chao LI, Fengyuan HE, Xiaohui QI, Honghai YU, Jia DU a Dexin WANG. Study on Flow Field Optimization of SCR Denitrification Reactor Based on CFD Numerical Simulation Technology. *IOP Conference Series: Earth and Environmental Science* [online]. 2019, **242** [cit. 2022-04-26]. ISSN 1755-1315. Available from: doi:10.1088/1755-1315/242/4/042009
  8. MEHDI, Ghazanfar, Song ZHOU, Yuanqing ZHU, Ahmer SHAH a Kishore CHAND. Numerical Investigation of SCR Mixer Design Optimization for Improved Performance. *Processes* [online]. 2019, **7**(3) [cit. 2022-04-26]. ISSN 2227-9717. Available from: doi:10.3390/pr7030168
  9. KURZYDYM, Damian, Adam KLIMANEK a Zbigniew ŻMUDKA. Experimental research and CFD analysis of flow parameters in a SCR system for the original part and WALKER's replacement. *Combustion*

- Engines* [online]. 2019, **179**(4), 13-20 [cit. 2022-04-26]. ISSN 2300-9896. Available from: doi:10.19206/CE-2019-402
10. HOLTZ, Dorian, Conrad GIEROW, Robert BANK, Dirk KADAU a Flavio SOPPELSA. CFD simulation of particle deposition in exhaust gas treatment systems. SIEBENPFEIFFER, Wolfgang, ed. *Heavy-Duty-, On- und Off-Highway-Motoren 2019* [online]. Wiesbaden: Springer Fachmedien Wiesbaden, 2020, s. 69-82 [cit. 2022-04-26]. Proceedings. ISBN 978-3-658-31370-8. Available from: doi:10.1007/978-3-658-31371-5\_6
  11. WARDANA, Muhammad Khristamto Aditya, G. M. Hasan SHAHARIAR, Kwangchul OH a Ocktaeck LIM. Ammonia Uniformity to Predict NOx Reduction Efficiency in an SCR System. *International Journal of Automotive Technology* [online]. 2019, **20**(2), 313-325 [cit. 2022-04-26]. ISSN 1229-9138. Available from: doi:10.1007/s12239-019-0031-x
  12. LUO, Zhaoyu, Parvez SUKHESWALLA, Scott A. DRENNAN, Mingjie WANG a P. K. SENEAL. 3D Numerical Simulations of Selective Catalytic Reduction of NOx With Detailed Surface Chemistry. In: *Volume 2: Emissions Control Systems; Instrumentation, Controls, and Hybrids; Numerical Simulation; Engine Design and Mechanical Development* [online]. American Society of Mechanical Engineers, 2017, s. - [cit. 2022-04-26]. ISBN 978-0-7918-5832-5. Available from: doi:10.1115/ICEF2017-3658
  13. LEE, Changhee. Numerical and experimental investigation of evaporation and mixture uniformity of urea–water solution in selective catalytic reduction system. *Transportation Research Part D: Transport and Environment* [online]. 2018, **60**, 210-224 [cit. 2022-04-26]. ISSN 13619209. Available from: doi:10.1016/j.trd.2017.04.015
  14. ZHANG, Chaofeng, Chuan SUN, Meiping WU a Kai LU. Optimisation design of SCR mixer for improving deposit performance at low temperatures. *Fuel* [online]. 2019, **237**, 465-474 [cit. 2022-04-26]. ISSN 00162361. Available from: doi:10.1016/j.fuel.2018.10.025
  15. GAO, Xiang, Ben WANG, Xudong YUAN, Siyuan LEI, Qinggong QU, Chuan MA a Lushi SUN. Optimal design of selective catalyst reduction denitrification system using numerical simulation. *Journal of Environmental Management* [online]. 2019, **231**, 909-918 [cit. 2022-04-26]. ISSN 03014797. Available from: doi:10.1016/j.jenvman.2018.10.060
  16. NOVÁK, Martin a Richard MATAS. *Numerical simulation of flue gas in selective catalytic reduction system* [online]. In: . s. 040003- [cit. 2022-04-26]. Available from: doi:10.1063/5.0041560



17. BLEJCHAŘ, Tomáš. *Turbulence modelového proudění - CFX: učební text*. Vyd. 1. Ostrava: Vysoká škola báňská - Technická univerzita Ostrava, 2012. ISBN 978-80-248-2606-6.
18. KOZUBKOVÁ, Milada. *Modelování proudění tekutin FLUENT, CFX* [online]. 1. vyd. Ostrava: Vysoká škola báňská - Technická univerzita, 2008 [cit. 2022-04-26]. ISBN 978-80-248-1913-6.
19. PINKUS, Oscar a Beno STERNLICHT. *Theory of hydrodynamic lubrication*. New York: McGraw-Hill, 1961.
20. ANSYS *Fluent User's Guide 2021 R1* [PDF]. 2021. U.S.A., 2021 [cit. 2022-04-26].
21. MENTER, F. Zonal Two Equation k-w Turbulence Models For Aerodynamic Flows. In: *23rd Fluid Dynamics, Plasmadynamics, and Lasers Conference* [online]. Reston, Virigina: American Institute of Aeronautics and Astronautics, 1993, s. - [cit. 2022-04-26]. Available from: doi:10.2514/6.1993-2906
22. WELTENS, Herman, Harald BRESSLER, Frank TERRES, Hubert NEUMAIER a Detlev RAMMOSER. *Optimisation of Catalytic Converter Gas Flow Distribution by CFD Prediction* [online]. In: . s. - [cit. 2021-12-20]. Available from: doi:10.4271/930780
23. SUN, Ke, Haiyang ZHAO, Kui ZHAO, Da LI a Shuzhan BAI. Optimization of SCR inflow uniformity based on CFD simulation. *Open Physics* [online]. 2020, **18**(1), 1168-1177 [cit. 2021-12-20]. ISSN 2391-5471. Available from: doi:10.1515/phys-2020-0221
24. BRESSLER, H., D. RAMMOSER, H. NEUMAIER a F. TERRES. *Experimental and Predictive Investigation of a Close Coupled Catalytic Converter with Pulsating Flow* [online]. In: . s. - [cit. 2021-12-20]. Available from: doi:10.4271/960564
25. LU, Kai, Dewen LIU, Yan WU, Shusen LIU a Shuzhan BAI. A study on the high-efficiency mixer of the SCR system. *Mechanics & Industry* [online]. 2021, **22** [cit. 2021-12-20]. ISSN 2257-7777. Available from: doi:10.1051/meca/2020101
26. MCKINLEY, Thomas L., Andrew G. ALLEYNE a Chia-Fon LEE. Mixture Non-Uniformity in SCR Systems: Modeling and Uniformity Index Requirements for Steady-State and Transient Operation. *SAE International Journal of Fuels and Lubricants* [online]. 2010, **3**(1), 486-499 [cit. 2021-12-20]. ISSN 1946-3960. Available from: doi:10.4271/2010-01-0883
27. CAPETILLO, Azael J., Fernando IBARRA, Dominik STEPNIEWSKI a Jo VANKAN. Multiphase Modelling of SCR Systems: Using the Taguchi Method for Mixer Optimisation. *SAE International Journal of*

- Engines* [online]. 2017, **10**(1), 61-71 [cit. 2021-12-20]. ISSN 1946-3944. Available from: doi:10.4271/2017-26-0113
28. VEDAGIRI, Praveena, Leenus Jesu MARTIN a Edwin Geo VARUVEL. Characterization of urea SCR using Taguchi technique and computational methods. *Environmental Science and Pollution Research* [online]. 2021, **28**(10), 11988-11999 [cit. 2021-12-03]. ISSN 0944-1344. Available from: doi:10.1007/s11356-020-08743-y
29. GIRARD, James W., Figen LACIN, Charles J. HASS a Joseph HODONSKY. *Flow Uniformity Optimization for Diesel Aftertreatment Systems* [online]. In: . s. - [cit. 2021-12-20]. Available from: doi:10.4271/2006-01-1092
30. JOHANSSON, Åsa, Ulf WALLIN, Mikael KARLSSON, Annika ISAKSSON a Phillip BUSH. *Investigation on Uniformity Indices Used for Diesel Exhaust Aftertreatment Systems* [online]. In: . s. - [cit. 2021-12-20]. Available from: doi:10.4271/2008-01-0613